

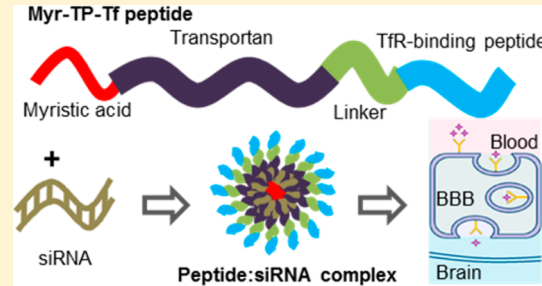
A Myristoylated Cell-Penetrating Peptide Bearing a Transferrin Receptor-Targeting Sequence for Neuro-Targeted siRNA Delivery

Pilju Youn, Yizhe Chen, and Darin Y. Furgeson*

Department of Pharmaceutics and Pharmaceutical Chemistry, University of Utah, Salt Lake City, Utah 84112, United States

ABSTRACT: Many neurodegenerative disorders (NDDs) are characterized by aggregation of aberrant proteins and extensive oxidative stress in brain cells. As a treatment option for NDDs, RNA interference (RNAi) is a promising approach to suppress the activation of abnormal genes and negative regulators of antioxidant genes. Efficient neuro-targeted siRNA delivery requires a delicate optimization of nucleic acid carriers, quite distinct from putative pDNA carriers in regard to stable condensation and serum protection of siRNA, blood–brain barrier (BBB) bypass, effective siRNA delivery to brain cells, and functional release of bioactive siRNA at therapeutic levels. Here, we propose that a myristic acid conjugated, cell-penetrating peptide (transportan; TP), equipped with a transferrin receptor-targeting peptide (myr-TP-Tf), will lead to stable encapsulation of siRNA and targeted delivery of siRNA to brain cells overcoming the BBB. Myr-TP-Tf was successfully prepared by solid-phase peptide synthesis with high purity. Myr-TP-Tf–siRNA complexes formulated at a 20:1 (peptide–siRNA) molar ratio provided prolonged siRNA stability against serum and ribonuclease treatment. Fluorescence images clearly indicated that siRNA uptake was successfully achieved by myr-TP-Tf complexes in both a murine brain endothelioma and a human glioma cell line. The luciferase assay and the human placental alkaline phosphatase (hPAP) reporter assay results demonstrated the functional gene silencing effect of myr-TP-Tf–siRNA complexes in a human glioma cell line as well as in primary murine neurons/astrocytes, supportive of successful release of bioactive siRNA into the cytosol. Finally, the transcytosis assay revealed that favorable siRNA transport via receptor-mediated transcytosis was mediated by myr-TP-Tf complexes. In summary, these data suggest that myr-TP-Tf peptides possess promising properties as a vehicle for neuro-targeted siRNA delivery. We will further study this peptide *in vitro* and *in vivo* for transport mechanism kinetics and to validate its capability to deliver siRNA to the brain, respectively.

KEYWORDS: siRNA carrier, cell-penetrating peptide, blood–brain barrier (BBB), transferrin receptor, receptor-mediated transcytosis, neuro-targeting, neurodegenerative disorders (NDDs)



1. INTRODUCTION

Today, neurodegenerative disorders (NDDs) are a critical, rising major health concern across the globe, a burgeoning pandemic of dementia encompassing Alzheimer's disease (AD), Parkinson's disease (PD), amyotrophic lateral sclerosis (ALS), and Huntington's disease (HD). Based on the growing trend of the aged population, it is estimated that approximately 115 million people will suffer from NDDs by 2050.¹ The health care cost for the treatment of NDDs is estimated to reach \$1.1 trillion by 2050 in the US alone.² Despite increasing incidences and enormous economic, social, and emotional burdens of NDDs, relatively few NDD therapeutics are clinically viable. This disparity is due in large part to the difficulties of drug delivery across the blood–brain barrier (BBB), which has prompted many pharmaceutical companies to abandon their neuropharmaceutical programs.^{3,4} Typically, the defensive brain vasculature allows passage of only small, hydrophobic compounds across the BBB because of the regulation provided by tight junction proteins found between endothelial cells. Hence, there is an acute need for drug delivery vehicles and/or biotherapeutic formulations to cross the BBB with favorable PK/PD.^{5,6}

Many NDDs are characterized by accumulation of abnormal proteins such as beta amyloid peptide ($A\beta$ 1–42) and tau proteins found in AD,⁷ α -synuclein in PD,⁸ and polyglutamine repeats in HD.⁹ Along with these protein aggregates, the elevated oxidative stress is also considered a key pathological factor for the onset and progression of NDDs.¹⁰ As a therapeutic option for NDDs, an RNA interference (RNAi) approach has the potential to suppress the abnormally regulated genes or any negative regulators of endogenous antioxidant genes. For instance, the Nrf2 (NF-E2-related factor 2)-Keap1 (kelch-like ECH-associated protein) pathway is a promising target as Nrf2 activates the expression of detoxifying and antioxidant genes, which relieves the oxidative stress.^{10–13} Because Nrf2 activity is normally restricted by Keap1, which sequesters Nrf2 in the cytoplasm and directs it to the proteasomal degradation pathway,^{14,15} it is expected that downregulation of the Keap1 protein using an RNAi approach

Received: July 30, 2013

Revised: December 3, 2013

Accepted: January 3, 2014

Published: January 3, 2014

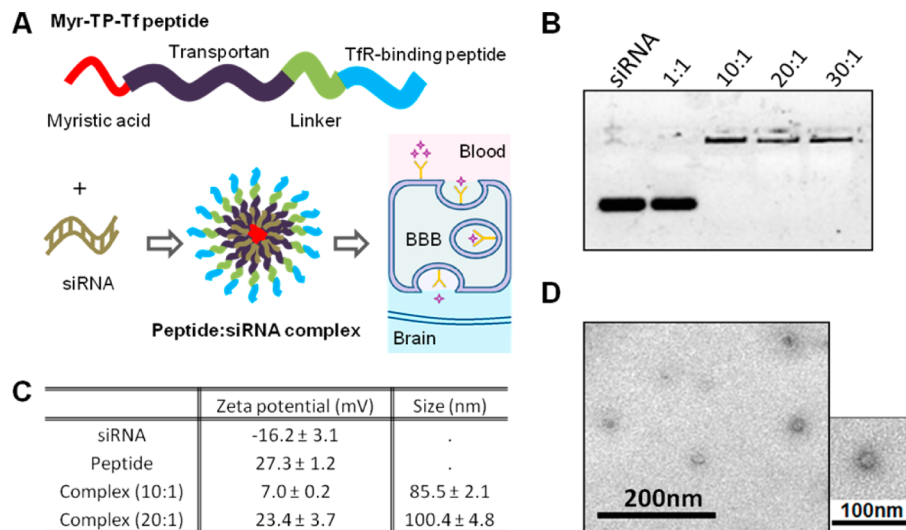


Figure 1. Design and characterization of myristoylated transportan peptide equipped with transferrin receptor targeting short peptide (myr-TP-Tf). (A) Illustration of myr-TP-Tf peptide and its postulated peptide–siRNA complex structure and expected brain-targeted siRNA delivery mechanism; (B) gel retardation assay, 0.8% agarose gel electrophoresis at 100 V for 20 min; and (C) zeta potential and particle size measurements ($n = 3/\text{group}$). Data reported as mean \pm standard error; and (D) transmission electron microscopy images of peptide–siRNA complexes (20:1 molar ratio).

will result in liberation and translocation of Nrf2 and subsequent expression of antioxidant genes, thereby providing cytoprotection to brain cells.

However, drug delivery, let alone neuro-targeted siRNA delivery, remains a daunting task. First, the negatively charged backbone of siRNA presents a hurdle for favorable cell membrane association. Plus, the naked siRNA has a short period of stability due to its susceptibility to serum nucleases.^{16,17} More crucially, the vascular endothelium of the BBB does not allow free passage from the systemic circulation to brain parenchyma. Therefore, successful brain-targeted siRNA transport requires formulations that fully condense siRNA *in vitro*, remain stable *in vivo*, and delivery vehicles that deposit a bioactive, therapeutic level of siRNA without undue toxicity at the targeted site. Diverse siRNA delivery platforms have been attempted including: chemically modified siRNA,¹⁸ polymeric nanoparticles,^{19,20} liposomes or exosomes,^{21,22} antibody-fusion molecules,²³ and cholesterol-conjugated siRNA.²⁴ For clinical application, however, currently investigated siRNA vehicles still require optimization regarding the physiological stability, BBB-targeting ability, and a functional RNAi effect.

To overcome the above listed obstacles, studies have indicated that cationic peptide repeats effectively encapsulate siRNA through electrostatic interactions^{25–28} and also facilitate the cellular uptake of nucleic acid.^{29,30} Thus, it is conceivable that siRNA carriers comprised of a cationic domain fused with a BBB-targeting group should be capable of siRNA condensation and delivery across the BBB. Kumar et al. presented transvascular delivery of siRNA to neurons using synthetic oligo-arginine peptides linked with a rabies virus glycoprotein (RVG)-derived domain that binds to acetylcholine receptors on neuronal cells.³¹ This finding provided an encouraging basis for the development of neuro-targeted, peptide-based siRNA carriers. In a recent study, various cell-penetrating peptides were characterized and evaluated in regard to effective siRNA delivery to tumor cells; the myristoylated transportan peptide was identified as the most suited showing a 2-fold higher fitness in knockdown efficiency than the TAT cell penetrating

peptide.³² Myristylation of the cell-penetrating peptide is also a beneficial strategy for carrier design, as it is known to enhance the peptide affinity for the cellular membrane.^{33–35} Another study showed that myristoylated polyarginine peptides mediated efficient siRNA internalization to brain cells *in vitro*,³⁶ but the physiological performance *in vivo* may not be ensured without an adequate neuro-targeted moiety.

In the current work, we designed a BBB-targeting siRNA carrier exploiting the N-terminally myristoylated transportan peptide as a cell-penetrating and siRNA condensation domain and a transferrin receptor-targeting 12 amino acid sequence (THRPPMWSPVWP)^{37,38} as a BBB-targeting domain. We hypothesized that a myristic acid conjugated, cell-penetrating peptide (transportan) equipped with a transferrin receptor-targeting peptide (myr-TP-Tf) would enable the stable condensation of siRNA and facilitate targeted delivery of siRNA to brain cells through receptor-mediated transcytosis as illustrated in Figure 1A. The data from *in vitro* studies here confirmed that the myr-TP-Tf peptide formed stable peptide–siRNA complexes and achieved superior siRNA uptake in brain endothelial cells and glioma cells when compared to putative lipofectamine–siRNA controls or nontargeted (scrambled) peptide–siRNA controls. In addition, myr-TP-Tf–siRNA complexes displayed the functional, reporter protein knockdown without affecting cell viability and favorable siRNA transport across a model, brain endothelial cell monolayer.

2. EXPERIMENTAL SECTION

2.1. Peptide Synthesis. The myristic acid conjugated, cell-penetrating peptide (transportan) equipped with a transferrin receptor-targeting peptide (myr-TP-Tf) and its nontargeting scrambled control peptide (myr-TP-Scr) were prepared by solid-phase peptide synthesis at Selleckchem (Houston, TX). The peptide sequences for myr-TP-Tf and myr-TP-Scr are as follows: myristic acid-GWTLNSAGYLLGKINLKALA-ALAKKIL-GGGG-THRPPMWSPVWP and myristic acid-GWTLNSAGYLLGKINLKALAALAKKIL-GGGG-PWRP-SHPVWMPT, respectively. The purity (>95%) and the molecular weight (4.5 kDa) of the peptides were confirmed

by high-performance liquid chromatography (HPLC) and mass spectrometry analyses upon receipt.

2.2. Formulation of siRNA–Carrier Complexes and Gel Retardation Assay. Myr-TP-Tf peptide was mixed with 20 pmol of siRNA at different molar ratios ranging from 1:1 to 10:1, 20:1, and 30:1 (peptide–siRNA) in distilled water. Samples were vortexed for 20 s and incubated for 20 min at room temperature. Each sample was mixed with 6× DNA loading dye (Fermentas, Hanover, MD) and subjected to 0.8% agarose gel electrophoresis for 20 min at 100 V. Bands were stained with SYBR Green II RNA gel stain (Invitrogen, Carlsbad, CA) and visualized under UV light.

2.3. Transmission Electron Microscopy. The morphology of the myr-TP-Tf–siRNA complexes was examined by transmission electron microscopy (TEM). Briefly, 20 μL of the peptide–siRNA complex solution (20:1 molar ratio, 20 μM of siRNA) was loaded on carbon-coated, copper electron microscopy grids and air-dried for one hour. The peptide–siRNA complexes were negatively stained with 2% phosphotungstic acid for 30 s, and the excess liquid was wicked away with a tip of filter paper. The grids were then examined by a 120 kV Tecnai 12 TEM (FEI, Hillsboro, OR) at the electron microscopy lab in the University of Utah HSC Core Research Facility.

2.4. Particle Size and Zeta Potential Measurement. The myr-TP-Tf–siRNA complexes were prepared in either 10:1 or 20:1 molar ratio in distilled water (100 nM of siRNA). The hydrodynamic diameter and the surface charge of the complexes were determined by using a Zetasizer Nano ZS (Malvern Inc., Westborough, MA). All measurements were collected in triplicate and expressed as mean ± standard errors. Each measurement consisted of at least 11 runs.

2.5. Examination of siRNA Stability against Fetal Bovine Serum and Ribonuclease A. Naked siRNA and myr-TP-Tf–siRNA complexes were incubated in 50% fetal bovine serum at 37 °C. Aliquots were collected at 0, 30 min, 4 h, 8 h, and 24 h of incubation and frozen for storage. Each sample was then treated with proteinase K (1 mg/mL) at 37 °C for 10 min. To evaluate the siRNA protection against RNase A, naked siRNA and myr-TP-Tf–siRNA complexes were incubated in RNase A solution (0.04 mg/mL) at 37 °C for 0, 30 min, 1 h, 2 h, and 4 h and treated with 2 μL of 10 M NaOH solution to disrupt the complex structures. All samples were mixed with 6× DNA loading dye and subject to 0.8% agarose gel electrophoresis for 20 min at 100 V. The gels were stained with SYBR Green II RNA gel stain (Invitrogen) to examine the siRNA integrity under UV light.

2.6. Cell Culture: Human Glioma U87 mg and Murine Brain Endothelioma b.End3 Cell Lines. Human glioma U87 mg cells that constitutively express luciferase were kindly donated by Prof. Randy Jensen (University of Utah; Dept. of Neurosurgery) and maintained in Dulbecco's modified Eagle's medium (DMEM; Invitrogen) supplemented with 10% fetal bovine serum, 100 U/mL of penicillin/streptomycin, and 0.5 mg/mL of Geneticin selective antibiotic (G418 sulfate). During the transfection studies, G418 was not contained in the culture medium. Murine brain endothelioma b.End3 cells were purchased from ATCC (Manassas, VA) and maintained in DMEM supplemented with 10% fetal bovine serum and 100 U/mL of penicillin/streptomycin. The cell cultures were maintained in a humidified atmosphere containing 5% CO₂ at 37 °C.

2.7. Cell Culture: Primary Murine ARE–hPAP(+) Neurons/Astrocytes. The ARE–hPAP (antioxidant response element–human placental alkaline phosphatase) (+) transgenic mice were kindly gifted by Prof. Jeffrey Johnson (University of Wisconsin-Madison) and maintained in accordance with University of Utah IACUC guidelines. The mice were mated, and the mother mice were sacrificed at day 15 of pregnancy to isolate the E15 brain cortices from embryonic mice. The tissues were washed with Hank's buffer salt solution (HBSS; Invitrogen) and digested with 0.05% trypsin for 20 min at 37 °C. The cell suspensions were filtered through 70 μm cell strainers (BD Falcon, San Jose, CA) and plated at a density of 10⁵ cells/well on 96-well plates in EMEM supplemented with 10% fetal bovine serum (FBS), 10% horse serum, 2 mM of L-glutamine, and 100 U/mL of penicillin/streptomycin following the protocol established by the Johnson lab.³⁹ On day 2, the medium was replaced with neurobasal medium (Invitrogen) containing B27 supplements, 2 mM of L-glutamine, and 100 U/mL of penicillin/streptomycin. The primary neurons/astrocytes were cultured at 37 °C in a humidified trivas chamber (5% CO₂/5% O₂/90% N₂).

2.8. Cell Transfection. U87 mg-Luc cells were plated on 96-well plates with 10⁴ cells/well and grown to 70–80% confluence. The cells were transfected with peptide: luciferase siRNA complexes (4 pmol of siRNA/well) in DMEM without serum and antibiotics for 3 h and then incubated in complete culture medium for an additional 45 h. Lipofectamine RNAiMAX Reagent (Invitrogen) was used as the control transfection reagent following the manufacturer's protocol.

2.9. Immunocytochemistry for Transferrin Receptors. U87 mg cells and b.End3 cells were grown on 6-well plates up to 70% confluence. The cells were twice washed with ice-cold PBS and fixed with 4% paraformaldehyde for 15 min at room temperature. Following three additional rinses of PBS, the cells were incubated with a polyclonal, rabbit antibody to the transferrin receptor (Abcam Inc., Cambridge, MA) in PBS at 4 °C overnight. After washing the samples with ice-cold PBS three times 5 min each, the cells were incubated with Alexa Fluor 488 Goat Anti-Rabbit IgG (Invitrogen) for one hour and examined using an Olympus IX71F fluorescence microscope (Scientific Instrument Company, Aurora, CO).

2.10. Fluorescence Imaging of siRNA Uptake. To examine the siRNA uptake by U87 mg cells and b.End3 cells, siGLO RNA-induced silencing complex (RISC)-free control siRNA labeled with Dy547 fluorescent dye (Thermo Scientific, Rockford, IL) was used to formulate peptide–siRNA complexes. The cells were grown on 6-well plates to 70% confluence and each well subsequently treated with 100 pmol of siRNA in either a naked or a peptide–siRNA complex form in DMEM for 3 h and washed with PBS three times. The fluorescence images were acquired by using an Olympus IX71F fluorescence microscope, and the red fluorescence color was added to the acquired images by Image J software (NIH Image, Bethesda, MD).

2.11. Cellular Luciferase Assay Expression for an Examination of the Functional Gene Silencing Effect. Upon 48 h of incubation after transfecting luciferase siRNA, the U87 mg-Luc cells were washed with PBS and lysed in a passive lysis buffer (Promega, Madison, WI) for 15 min. A sample of 20 μL of the lysates were transferred to a white 96-well plate and 100 μL of luciferase assay reagent (Promega) was added per well. After two min of dark incubation, the luminescence intensity from each well was measured using a PlateLumino

Luminometer (Stratec Biomedical Systems, Birkenfeld, Germany). The total protein amount was quantified by a BCA assay to correct the luminescence intensity per milligram of protein.

2.12. Human Placental Alkaline Phosphatase (hPAP) Assay.

The hPAP assay was performed following the protocol established by Prof. Jeffrey Johnson (University of Wisconsin—Madison).³⁹ Briefly, the primary neurons/astrocytes were lysed in TMNC lysis buffer (0.05 M Tris, 0.005 M MgCl₂, 0.1 M NaCl, 1% 3-[3-cholamidopropyl] dimethylammonio]-1-propanesulfonate [CHAPS]) and incubated at 65 °C for 30 min in 0.2 M diethanolamine buffer. The CSPD (chemiluminescent substrates for alkaline phosphatase) and Emerald (luminescence enhancer) reagents from Applied Biosystems (Bedford, MA) were used as substrates to quantify the hPAP activity, and the luminescence intensity was measured using a luminometer. A BCA assay followed to normalize the hPAP activity to total protein.

2.13. Cell Viability Assay. Cell viability was determined by using a tetrazolium salt 3-(4,5-dimethylthiazol-2-yl)-5-(3-carboxymethoxyphenyl)-2-(4-sulfophenyl)-2H-tetrazolium salt (MTS) substrate—as per the cell proliferation kit (Promega) and following the manufacturer's instruction.

2.14. Transcytosis Assessment. b.End3 cells were seeded at a density of $6 \times 10^4/\text{cm}^2$ onto 12 mm Transwell inserts (polycarbonate membrane, 0.4 μm pore size, Corning, NY), and the cells at day 8 were used for experiments. The inserts were filled with 300 μL of DMEM and the bottom compartments with 500 μL of DMEM. 50 pmol of peptide-Dy547-labeled siRNA complexes were applied onto the b.End3-coated, transwell inserts and incubated in a 37 °C CO₂ incubator. To evaluate the siRNA transport, 200 μL of the medium was collected from the abluminal compartment 6 h postincubation. The fluorescence intensity from the aliquots was measured by using a microplate reader (Bio-Rad, Hercules, CA) with a wavelength setting 557/570 Ex/Em. The amount of transported siRNA was calculated from a standard curve generated from the fluorescence intensity of the known amount of Dy547-labeled siRNA. Transendothelial electrical resistance (TEER) was measured before and after the siRNA treatment to ensure the b.End3 cell monolayer integrity. The paracellular barrier integrity was additionally monitored by measuring the permeability coefficient of sodium fluorescein (376.3 Da). 10 μM of sodium fluorescein in Krebs-Ringer buffer was loaded to the insert well, and the abluminal medium aliquots were collected every 15 min over an hour to determine the diffused concentration.

2.15. Statistical Analysis. The data are expressed as mean ± standard errors and were statistically analyzed by conducting a one-way ANOVA followed by Tukey-Kramer HSD posthoc analysis. A Student's *t*-test was performed for the siRNA transport study. Statistical significance is indicated by asterisks (**p* < 0.05; ***p* < 0.01; ****p* < 0.001). JMP v10.0 (SAS Institute Inc., Cary, NC) was used for performing the statistical analyses, and the graphs were generated by SigmaPlot 10.0 (Systat, San Jose, CA).

3. RESULTS

3.1. Characterization of myr-TP-Tf Peptide. The myr-TP-Tf peptide was successfully synthesized with a high purity and precise molecular weight (data not shown). We first investigated the optimal molar ratio of myr-TP-Tf to siRNA at which the complexes would achieve stable electrostatic

condensation. The gel retardation assay revealed that the myr-TP-Tf peptide condensed siRNA beginning at a 10:1 molar ratio (Figure 1B). The hydrodynamic diameter and the surface charge were measured for the complexes formulated at 10:1 and 20:1 molar ratios (Figure 1C). The 10:1 complexes (85.5 ± 2.1 nm) displayed a relatively smaller size than the 20:1 complexes (100.4 ± 4.8 nm), which may be due to an increased association number (N_A) or number of peptides per complex. Experiments are ongoing to further elucidate this trend. The zeta potential of the 10:1 complexes (7.0 ± 0.2 mV) was less than the myr-TP-Tf itself, indicating that the cationic charge of myr-TP-Tf was shielded by the electrostatic interaction with the negatively charged siRNA backbone. The 20:1 complexes displayed a higher positive charge range (23.4 ± 3.7 mV) compared to the 10:1 complexes, which further substantiates our hypothesis of an increased N_A with complex formation. 30:1 or higher molar ratios were not included in this study as the excessive cationic charge induced potent cytotoxicity. The general morphology of the peptide–siRNA (20:1) was examined by TEM. The representative TEM images show that the complexes possess spherical structures, which was in accordance with expectations (Figure 1D). The size of the complexes was smaller (~30 nm) in the TEM images than the dynamic laser scattering measurements due to shrinkage under the anhydrous, vacuum environment.

3.2. Enhanced siRNA Stability. siRNA instability is a major concern for therapeutic RNAi application *in vivo*. We investigated the siRNA integrity in 50% FBS and RNase A solution to evaluate the siRNA protection ability of the peptide–siRNA complexes. It was observed that the siRNA in the complex form displayed prolonged stability showing at least partial stability for up to eight hours in 50% FBS, whereas the naked form of siRNA was nearly untraceable at the 4 h time point (Figure 2A). The siRNA protection capability of the complexes was more dramatic in the RNase A treatment assay. Over the 4 h incubation time, the siRNA band intensity of the complexes stayed nearly intact, while the naked siRNA immediately began to degrade (Figure 2B). Literature shows

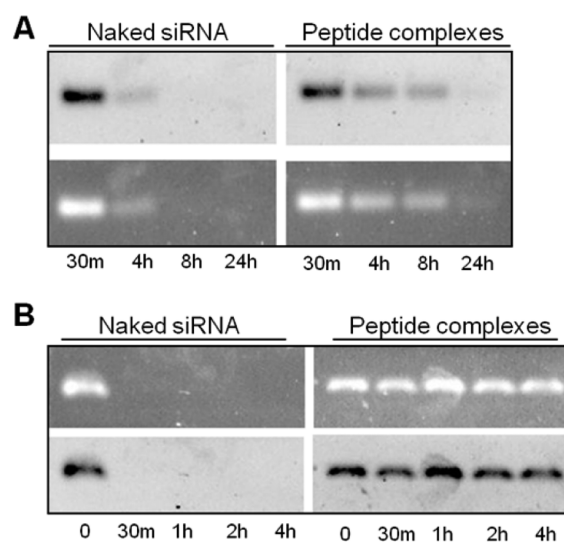


Figure 2. Comparison of siRNA stability: naked siRNA vs peptide–siRNA complex forms. (A) siRNA stability against 50% fetal bovine serum, 0.8% agarose gel electrophoresis at 100 V for 20 min and (B) siRNA stability against ribonuclease A, 0.8% agarose gel electrophoresis at 100 V for 20 min.

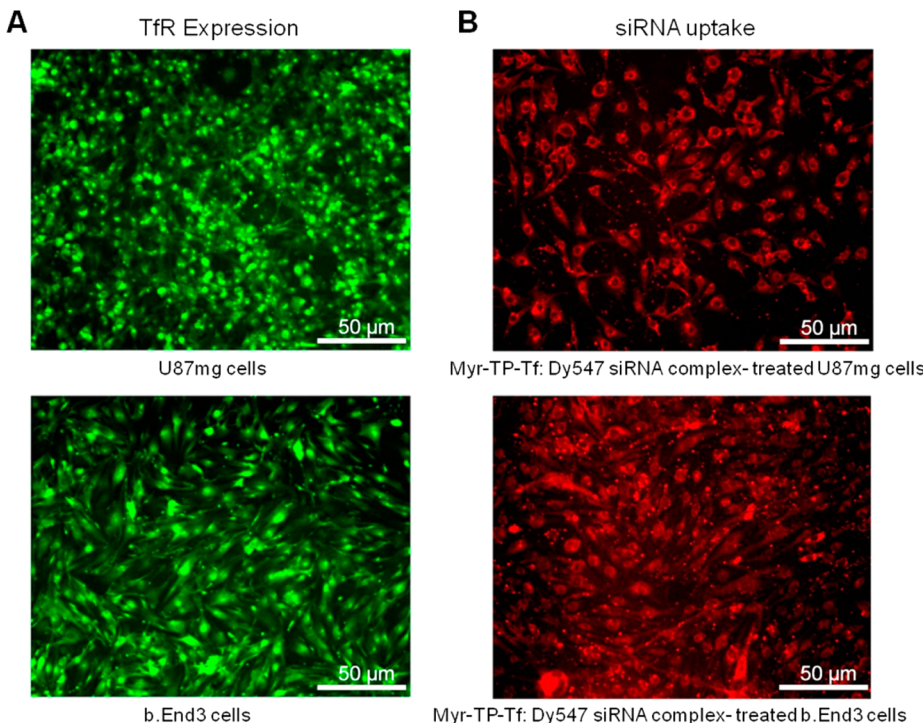


Figure 3. Verification of transferrin receptor expression and siRNA uptake in U87 mg and b.End3 cells. (A) Immunostaining of TfR on U87 mg cells (top) and on b.End3 cells (bottom) and (B) myr-TP-Tf-Dy547 siRNA complex-treated U87 mg cells (top) and b.End3 cells (bottom).

that even chemical modification of siRNA does not necessarily improve the gene silencing effect *in vivo*, despite the reported enhanced serum stability.¹⁶ From a clinical perspective, it would be imperative to achieve the therapeutic concentration at the target organ within a reasonable time frame in regard to the complexes' half-life.

3.3. Favorable siRNA Uptake. It is well-known that brain endothelial cells, neurons, and astrocytes express high levels of TfR proteins for transferrin-mediated iron supply, which is an essential cellular process for normal brain functions.⁴⁰ Prior to applying the myr-TP-Tf peptide, we completed immunostaining to verify the abundant expression of TfR on murine brain endothelial b.End3 and human glioma U87 mg cells used in this study. Representative images support the choice of TfR as a targeting receptor for both cell types (Figure 3A). However, nonspecific uptake by other organs of the complexes is expected upon *in vivo* administration because TfR proteins are ubiquitously expressed to varying extents. It should be noted that brain-targeting may not be exclusively achieved, but preferentially with the high levels of TfR existing on the brain endothelial cells.⁴¹ Next, siRNA uptake in b.End3 cells and U87 mg cells was examined to evaluate siRNA delivery capability of myr-TP-Tf peptides. To visualize siRNA internalization, Dy547 fluorescent dye-labeled siRNA was used in peptide–siRNA complex formulation. As shown in Figure 3B, b.End3 cells and U87 mg cells displayed intense red fluorescence after three hours of myr-TP-Tf–Dy547 siRNA complex incubation, indicating that the complexes successfully transported siRNA (Figure 3B) across the cell membrane barrier. To evaluate the targeting effect of the myr-TP-Tf peptide, b.End3 and U87 mg cells were treated with either naked Dy547 siRNA or nontargeted, myr-TP-Scr–Dy547 siRNA complexes. As anticipated, the naked Dy547 siRNA-treated group did not show detectable red fluorescence (Figure 4A). It was observed that the nontargeted control (scrambled) peptide complexes were

able to deliver siRNA to the cells (Figure 4B). This observation was not surprising because the control peptide also contains the cationic cell-penetrating peptide sequence and therefore has the same ability to condense siRNA. Compared to the targeting complexes, however, the extent of internalized siRNA was much less prominent, demonstrating that the enhanced cellular uptake of siRNA is possible when combined with a receptor-mediated pathway (Figure 4C).

3.4. Transfection of a Human Glioma Cell Line. Next, we investigated if the internalized siRNA functionally downregulates the target protein in brain cells. To this end, we used human glioma U87 mg-Luc cells which constitutively express luciferase. The U87 mg-Luc cells were treated with either naked siRNA targeting luciferase mRNA or peptide–luciferase siRNA complexes for three hours, and the luciferase activity was measured 45 h post-transfection. As shown Figure 5A, the luciferase-specific siRNA was successfully delivered to the U87 mg cells by myr-TP-Tf peptide complexes (20:1) and effectively silenced the luciferase mRNA, which is implicated in the significantly reduced luminescence intensity. The nontargeting peptide complexes (20:1) also resulted in a significant gene silencing effect to a certain degree. However, the extent of luciferase expression downregulation was not comparable to the levels produced by the targeting peptide, which complied with the different levels of cellular uptake of siRNA (Figure 4). The complexes prepared at a 10:1 molar ratio did not exert any significant RNAi effect. We hypothesize that the higher cationic surface charge and the multivalent presentation of targeting peptides account for the greater mRNA silencing effect of the 20:1 complexes, but we did not attempt higher ratios as we established higher molar ratios induce potent cytotoxicity. Throughout the transfection study, no significant cytotoxicity was observed from peptide–siRNA complex treatments (Figure 5B).

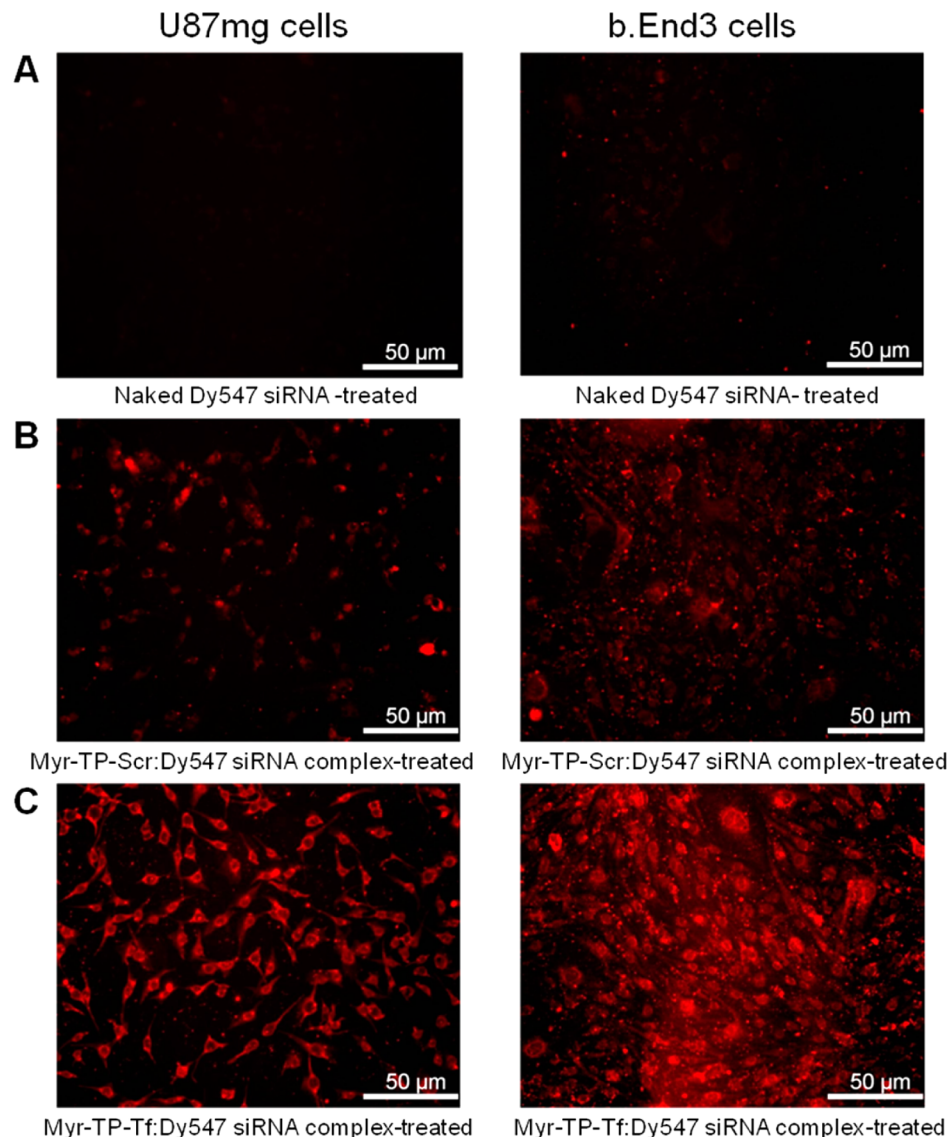


Figure 4. Enhanced siRNA uptake mediated by TfR-targeting peptide. (A) Naked Dy547-labeled siRNA-treated U87 mg (left) and b.End3 cells (right); (B) myr-TP-Scr-Dy547 siRNA complexes-treated U87 mg and b.End3 cells; and (C) myr-TP-Tf-Dy547 siRNA complexes-treated U87 mg and b.End3 cells.

3.5. Transfection of Primary Murine Neurons/Astrocytes. Primary cells are often considered generally difficult to transfect. To further validate the carrier transfection ability, primary murine neurons/astrocytes were extracted from brain cortices of E15 ARE:hPAP(+) transgenic mice, in which the hPAP reporter gene is inserted downstream of the ARE. As remarked in the Introduction, the Keap1-Nrf2 pathway is a promising target for the treatment of NDDs. It is expected that downregulation of Keap1 mRNA, using an RNAi approach, will result in liberation and translocation of Nrf2 to the nuclear ARE with subsequent activation of antioxidant genes, thereby providing cytoprotection to brain cells. ARE:hPAP(+) transgenic mice serve as a useful tool to examine the activation of ARE by analyzing the reporter hPAP activity. Here, primary murine neurons/astrocytes were transfected with myr-TP-TfR-siRNA complexes against Keap1 and the hPAP activity measured 48 h post-transfection. As shown in Figure 6A, the myr-TP-Tf-Keap1 siRNA complexes significantly induced hPAP activity (Figure 6A) as compared to the control groups. Again, the nontargeting peptide complexes also exhibited

positive transfection ability but to a lesser degree. As with the immortalized cell lines, the cell viability assay result indicated no significant cytotoxicity of the primary murine neurons/astrocytes (Figure 6B).

3.6. siRNA Transport Assay. The actual transport of the siRNA across brain endothelial cells was examined *in vitro* using a Transwell system in which b.End3 cells were grown as a confluent monolayer on inserts. We treated the inserts with 50 pmol of peptide-Dy547-labeled siRNA complexes for 6 h and assessed the transport of Dy547 siRNA by measuring the fluorescence intensity of the medium collected from the bottom compartments. The myr-TP-Tf-siRNA complexes treated group clearly showed an enhanced transport profile compared to the scrambled myr-TP-Scr-siRNA (Figure 7A). However, the transported siRNA quantity was less than the original amount, indicating that a significant portion of siRNA remained in the b.End3 cells monolayer over the 6 h. A naked siRNA-treated group was not included as the naked form of siRNA was not visibly taken up by b.End3 cells. To examine if the b.End3 cell monolayer remained intact during the transcytosis

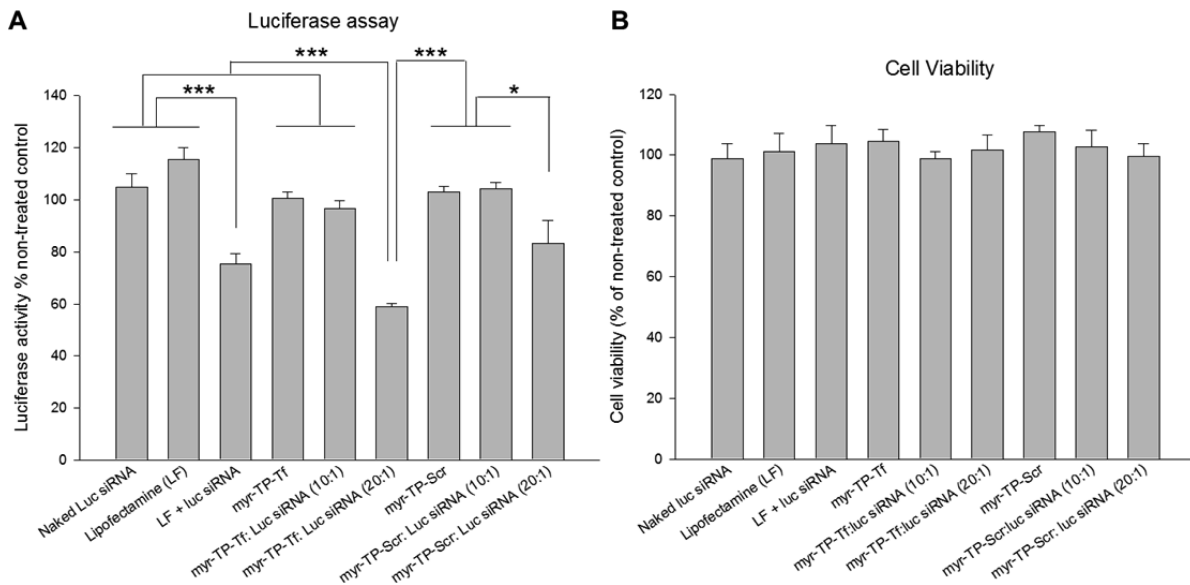


Figure 5. U87 mg-Luc glioma cells myr-TP-Tf-siRNA transfection. (A) Luciferase assay ($n = 5\text{--}7/\text{group}$) and (B) cell viability assay ($n = 5/\text{group}$) at 48 h post-transfection. Data are reported as the mean \pm standard error; one-way ANOVA with a Tukey-Kramer posthoc test was performed (* $p < 0.05$; ** $p < 0.01$; *** $p < 0.001$).

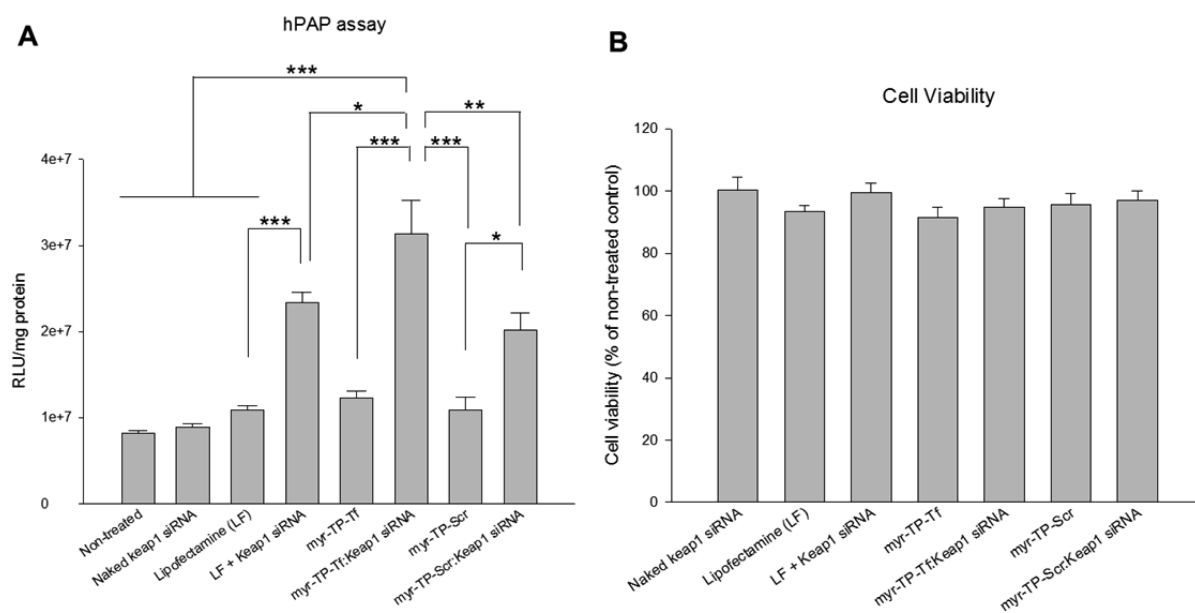


Figure 6. Transfection of myr-TP-Tf-Keap1 siRNA complexes to primary murine neurons/astrocytes. (A) Human placental alkaline phosphatase (hPAP) assay ($n = 6/\text{group}$) and (B) cell viability assay ($n = 5/\text{group}$) at 48 h post transfection. Data are reported as the mean \pm standard error; one-way ANOVA with Tukey-Kramer posthoc test was performed (* $p < 0.05$; ** $p < 0.01$; *** $p < 0.001$).

experiment, the TEER values before and after the siRNA treatments were compared, and no notable changes were detected (Figure 7B). The permeability coefficient of the water-soluble sodium fluorescein compound was additionally examined to evaluate the monolayer integrity. Even though it was higher [$(6.8 \pm 0.9) \cdot 10^{-6} \text{ cm/s}$] than the reported value from other *in vitro* BBB models established with primary rat brain endothelial cells [$(3.5 \pm 0.1) \cdot 10^{-6} \text{ cm/s}$],⁴² the order of magnitude of 10^{-6} cm/s is extremely small and considered an acceptable range for an *in vitro* BBB model.⁴³ Although the transported siRNA quantity over 6 h was found less than the loaded amount, it remains encouraging that the myr-TP-Tf complexes showed a promising siRNA transport property.

4. DISCUSSION

The physicochemical characteristics of myr-TP-Tf-siRNA complexes were in principle, well-suited for cell-targeted, *in vivo* administered RNAi. First, the myr-TP-Tf peptide successfully electrostatically condensed siRNAs with apparently optimal condensation in a reasonable range of peptide–siRNA molar ratios below the cytotoxic line of a 30:1 molar ratio. Second, the negative staining images of the peptide–siRNA complex under TEM revealed these complexes formed spherical structures, whereupon supramolecular self-assembly promoted core siRNA encapsulation in a core–shell architecture. The moderately positive surface charge of the complexes appeared to enhance complex interactions with

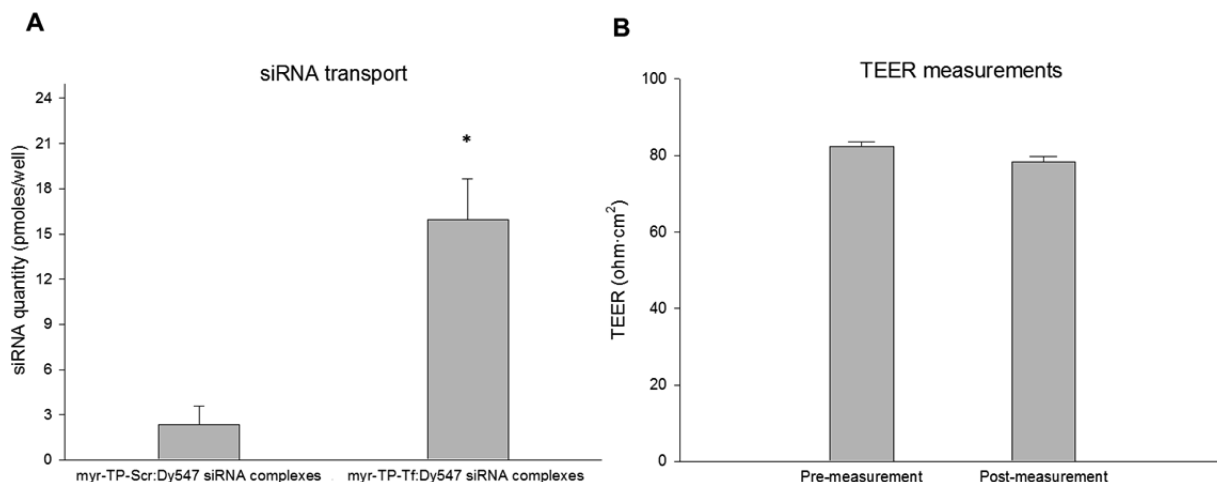


Figure 7. Assessment of siRNA transport across the b.End3 monolayer in a Transwell system 6 h after serum-free treatment. (A) Comparison of siRNA transport by myr-TP-Scr peptide–Dy547 siRNA complexes vs myr-TP-Tf–Dy547 siRNA complexes ($n = 3/\text{group}$). Student's *t* test was performed ($*p < 0.05$) and (B) TEER measurements before and after the transcytosis experiment ($n = 6/\text{group}$).

brain cells. It should be noted that the excessive cationic charge of nanoparticles normally involves detrimental effects to cells,⁴⁴ but these peptide–siRNA complexes did not arouse any notable cell viability changes to both the glioma cells and the primary murine brain cells within its measured and transfected surface charge range. Fourth, the particle size of the complexes was found to be fairly small considering that the siRNA molecule itself is quite bulky (14 kD). However, the particle size values measured in distilled water may not reflect the actual size in the culture medium or in the bloodstream. Indeed, when formulated in PBS (pH 7.4), the particle size was quite increased (230 ± 27.6 nm) while the surface charge was relatively maintained (28.6 ± 0.9 mV). It is likely that the ionic strength in buffer affects the tightness of the peptide–siRNA interaction leading to particle expansion.⁴⁵ Even with the increased diameter, the peptide–siRNA complexes did not show micrometer-sized aggregate formation. The imaging and the transfection results support that these complexes remain structurally viable for targeted cellular uptake and functional siRNA release in the brain cells.

In addition, the peptide–siRNA complexes were advantageous in regard to the siRNA stability in serum. The improved siRNA stability in the complexes also indicated that the siRNAs were protectively loaded within the complex structure. However, the *in vitro* serum stability testing may not present an accurate level of stability *in vivo*. This potential instability is a factor of the bloodstream itself, which may contain multiple nucleases in various ranges of concentration, resulting in dissimilar patterns of siRNA degradation kinetics.⁴⁶ Furthermore, it is plausible for these complexes to be entrapped by phagocytic cells and rapidly cleared from the bloodstream. Despite these multiple hurdles, an effective concentration of peptide–siRNA complexes should reach the brain, preserving bioactive siRNA integrity within the brain interstitial tissue while awaiting endo/transcytosis. In-depth studies elucidating the physiological stability needs and mechanisms of transport across the BBB are ongoing.

The transferrin receptor-targeting capacity of the complexes may raise questions because the nontargeting carrier with a scrambled sequence also showed the ability to deliver siRNA to the brain cells and exert some level of target gene silencing. For our purposes, we hypothesize that not only the targeting

moiety, but also the cationic surface charge on the complexes, plays a significant role for the cellular uptake of complexes. At a lower molar ratio (10:1), even for the TP-targeted carrier, no significant RNAi effect was observed, which may be the outcome from an insufficient cationic charge to interact with the cell membrane and/or the lack of targeting moieties presented to the cell receptors. Nevertheless, the targeted complexes formulated at a seemingly optimal (20:1) molar ratio showed preferential siRNA uptake and more significant target gene knockdown compared to nontargeted complexes at the same molar ratio. These data suggest that the receptor targeting ability provides an added effect for enhanced siRNA delivery. The siRNA transport results from the Transwell system also substantiate the benefit of the Tfr-targeting peptide sequence in the siRNA carrier. To achieve the highly selective targeting and thereby avoid the adverse effects from the nonspecific binding, further research efforts are required to find the optimal receptor candidates and identify their ligand binding modes.

In the siRNA transport assay, the targeting complexes also showed the more favorable siRNA transport to the abluminal compartment compared to the nontargeting complexes. However, this result may not be directly translatable to the *in vivo* condition; it should be noted that the *in vitro* BBB model used in our study is limitedly simulating the physiological BBB. Although the b.End3 cells can grow as a monolayer on the transwell insert membrane and express various tight junction proteins, the tightness of the monolayer, usually represented as TEER, never attains the values obtained from the *in vivo* BBB.⁴⁷ Being aware of the limitation, we conducted the experiments when the b.End3 cells formed a morphologically mature monolayer and the TEER values reached the fairly stable level. To exclude the possibility of any free Dy547 dye existence, HPLC-purified siRNAs were used, and the siRNA integrity was further examined on a couple of polyacrylamide gels before any assay. Though the b.End3 cells grown in a Transwell system may not be the most desirable surrogate for the physiological BBB, it served as a convenient tool to readily examine the complex ability to transport siRNA. Again, further complete examination for the siRNA transport should be followed by testing complexes in animal models.

As our studies were executed only *in vitro*, the *in vivo* performance of the complexes is therefore not yet guaranteed even with the promising properties. One reasonable question is that this single delivery system may not achieve the two, seminal intracellular trafficking processes: (i) receptor-mediated transcytosis across the BBB and (ii) subsequent cytosolic and/or transcytotic release of therapeutic levels of bioactive siRNA in the brain parenchyma. Transport mechanism studies are beyond the scope of this manuscript; however, the data are encouraging, and similar peptide-based delivery systems have shown levels of brain-targeted siRNA delivery and RNAi in the mouse brain.^{31,36} These authors did not provide detailed explanation of proposed transport mechanisms; however, again, these studies remain encouraging for peptide-mediated siRNA delivery across the BBB. Our goal is to achieve neuro-targeted siRNA delivery following systemic administration of the complexes. However, we recognize the established difficulties of peptide-mediated, systemically administered, targeted drug delivery let alone the complicated issues surrounding the applicability and relevance of RNAi therapy when compared to small molecule therapies. We remain optimistic as RNAi therapy remains a potent mode of treatment, yet continues to provide exciting challenges for therapeutic efficacy. Systemic administration may be overcome by alternative routes, such as local, intrathecal, or nasal delivery to avoid prolonged serum exposure, RES clearance, and inefficient neuro-targeting. Nasal delivery, with its readily accessible pathways to the BBB is a viable option,⁴⁸ avoiding the invasive complications of local delivery. Regardless, stable siRNA complexes with cell- or tissue-targeting capability to deliver bioactive and therapeutic levels of RNAi without compromising cell viability remain the key components in continued advancement of the RNAi field.

To conclude, the myr-TP-Tf peptide shows stable siRNA condensation and protection capability against serum and RNase A. Moreover, the novel peptide construct successfully delivered siRNA in amounts that significantly reduced reporter luciferase levels beyond that of the established, industrial siRNA-delivery vehicle of Lipofectamine in immortalized and primary cell lines. When combined, the data present an encouraging basis for continued exploration of the peptide *in vitro* and *in vivo*. In future work, we plan to use a fluorescently labeled peptide to better understand the exact transport mechanism(s) *in vitro* and *in vivo*. It will also elucidate the biodistribution pattern and neuro-targeting ability of the peptide in a living system. The successful completion of preclinical studies will ultimately provide a promising strategy for therapeutic siRNA delivery to brain tissues, which may be useful for treating or relieving the symptoms of various NDDs and numerous other brain maladies.

AUTHOR INFORMATION

Corresponding Author

*E-mail: darin.furgeson@gmail.com. Address: Nexus CMF, 2825 E Cottonwood Parkway #330, Salt Lake City, Utah 84121-7088. Phone: 1 801 657-4865. Fax: 1 801 702-8585.

Notes

The authors declare no competing financial interest.

ACKNOWLEDGMENTS

We appreciate Prof. Jeffrey Johnson (University of Wisconsin-Madison) for kindly providing the ARE-hPAP transgenic mice and Prof. Randy Jensen for sharing the trigas cell culture

chamber and U87 mg-Luc cell stocks. This work was supported by the NIH (1R21NS064541-01A1) and University of Utah start-up funds.

REFERENCES

- Batsch, N. L.; Mittelman, M. S. World Alzheimer report 2012. Overcoming the stigma of dementia. Alzheimer's disease international. Available at: <http://www.alz.co.uk/research/WorldAlzheimerReport2012.pdf> (accessed March 11, 2013).
- Thies, W.; Bleiler, L. Alzheimer's disease facts and figures. *Alzheimers Dement.* 2011, 7, 208–244.
- Abbott, N. J.; Rönnbäck, L.; Hansson, E. Astrocyte–endothelial interactions at the blood–brain barrier. *Nat. Rev. Neurosci.* 2006, 7, 41–53.
- Pardridge, W. M. Blood-brain barrier biology and methodology. *J. Neurovirol.* 1999, 5, 556–569.
- Pavan, B.; Dalpiaz, A.; Ciliberti, N.; Biondi, C.; Manfredini, S.; Vertuani, S. Progress in drug delivery to the central nervous system by the prodrug approach. *Molecules* 2008, 13, 1035–1065.
- Groothuis, D. R. The blood-brain and blood-tumor barriers: a review of strategies for increasing drug delivery. *Neuro-Oncology* 2000, 2, 45–59.
- Tiraboschi, P.; Hansen, L.; Thal, L.; Corey-Bloom, J. The importance of neuritic plaques and tangles to the development and evolution of AD. *Neurology* 2004, 62, 1984–1989.
- Braak, H.; Tredici, K. D.; Rüb, U.; de Vos, R. A.; Jansen Steur, E. N.; Braak, E. Staging of brain pathology related to sporadic Parkinson's disease. *Neurobiol. Aging* 2003, 24, 197–211.
- Scherzinger, E.; Sittler, A.; Schweiger, K.; Heiser, V.; Lurz, R.; Hasenbank, R.; Bates, G. P.; Lehrach, H.; Wanker, E. E. Self-assembly of polyglutamine-containing huntingtin fragments into amyloid-like fibrils: implications for Huntington's disease pathology. *Proc. Natl. Acad. Sci.* 1999, 96, 4604–4609.
- Melo, A.; Monteiro, L.; Lima, R. M. F.; de Cerqueira, M. D. Oxidative stress in neurodegenerative diseases: mechanisms and therapeutic perspectives. *Oxid. Med. Longev.* 2011, 2011, 1–14.
- Motohashi, H.; Yamamoto, M. Nrf2-Keap1 defines a physiologically important stress response mechanism. *Trends. Mol. Med.* 2004, 10, 549–557.
- Barnham, K. J.; Masters, C. L.; Bush, A. I. Neurodegenerative diseases and oxidative stress. *Nat. Rev. Drug Discovery* 2004, 3, 205–214.
- Calkins, M. J.; Johnson, D. A.; Townsend, J. A.; Vargas, M. R.; Dowell, J. A.; Williamson, T. P.; Kraft, A. D.; Lee, J. M.; Li, J.; Johnson, J. A. The Nrf2/ARE pathway as a potential therapeutic target in neurodegenerative disease. *Antioxid. Redox. Signal.* 2009, 11, 497–508.
- Itoh, K.; Wakabayashi, N.; Katoh, Y.; Ishii, T.; Igashiki, K.; Engel, J. D.; Yamamoto, M. Keap1 represses nuclear activation of antioxidant responsive elements by Nrf2 through binding to the amino-terminal Neh2 domain. *Gene. Dev.* 1999, 13, 76–86.
- Kobayashi, M.; Yamamoto, M. Molecular mechanisms activating the Nrf2-Keap1 pathway of antioxidant gene regulation. *Antioxid. Redox. Signal.* 2005, 7, 385–394.
- Layzer, J. M. M.; McCaffrey, A. P.; Tanner, A. K.; Huang, Z.; Kay, M. A.; Sullenger, B. A. In vivo activity of nuclease-resistant siRNAs. *RNA* 2004, 10, 766–771.
- Turner, J. J.; Jones, S. W.; Moschos, S. A.; Lindsay, M. A.; Gait, M. J. MALDI-TOF mass spectral analysis of siRNA degradation in serum confirms an RNase A-like activity. *Mol. Biosyst.* 2006, 3, 43–50.
- Nakajima, H.; Kubo, T.; Semi, Y.; Itakura, M.; Kuwamura, M.; Izawa, T.; Azuma, Y.-T.; Takeuchi, T. A rapid, targeted, neuron-selective, *in vivo* knockdown following a single intracerebroventricular injection of a novel chemically modified siRNA in the adult rat brain. *J. Biotechnol.* 2012, 157, 326–333.
- Chen, C.; Mei, H.; Shi, W.; Deng, J.; Zhang, B.; Guo, T.; Wang, H.; Hu, Y. EGFP-EGF1-conjugated PLGA nanoparticles for targeted delivery of siRNA into injured brain microvascular endothelial cells for efficient RNA interference. *PLoS One* 2013, 8, e60860.

- (20) Malmo, J.; Sandvig, A.; Vårum, K. M.; Strand, S. P. Nanoparticle mediated p-glycoprotein silencing for improved drug delivery across the blood-brain barrier: a siRNA-chitosan approach. *PLoS One* **2013**, *8*, e54182.
- (21) Alvarez-Erviti, L.; Seow, Y.; Yin, H. F.; Betts, C.; Lakhal, S.; Wood, M. J. A. Delivery of siRNA to the mouse brain by systemic injection of targeted exosomes. *Nat. Biotechnol.* **2011**, *29*, 341–345.
- (22) Tao, Y.; Han, J.; Dou, H. Brain-targeting gene delivery using a rabies virus glycoprotein peptide modulated hollow liposome: bio-behavioral study. *J. Mater. Chem.* **2012**, *22*, 11808–11815.
- (23) Xia, C. F.; Zhang, Y.; Boado, R. J.; Pardridge, W. M. Intravenous siRNA of brain cancer with receptor targeting and avidin–biotin technology. *Pharm. Res.* **2007**, *24*, 2309–2316.
- (24) Kuwahara, H.; Nishina, K.; Yoshida, K.; Nishina, T.; Yamamoto, M.; Saito, Y.; Piao, W.; Yoshida, M.; Mizusawa, H.; Yokota, T. Efficient in vivo delivery of siRNA into brain capillary endothelial cells along with endogenous lipoprotein. *Mol. Ther.* **2011**, *19*, 2213–2221.
- (25) Wang, Y. H.; Hou, Y. W.; Lee, H. J. An intracellular delivery method for siRNA by an arginine-rich peptide. *J. Biochem. Biophys. Methods* **2007**, *70*, 579–586.
- (26) Leng, Q.; Goldgeier, L.; Zhu, J.; Cambell, P.; Ambulos, N.; Mixson, A. J. Histidine-lysine peptides as carriers of nucleic acids. *Drug News Perspect.* **2007**, *20*, 77.
- (27) Deshayes, S.; Morris, M.; Divita, G.; Heitz, F. Cell-penetrating peptides: tools for intracellular delivery of therapeutics. *Cell. Mol. Life Sci.* **2005**, *62*, 1839–1849.
- (28) Gupta, B.; Levchenko, T. S.; Torchilin, V. P. Intracellular delivery of large molecules and small particles by cell-penetrating proteins and peptides. *Adv. Drug Delivery Rev.* **2005**, *57*, 637–651.
- (29) Wender, P. A.; Mitchell, D. J.; Pattabiraman, K.; Pelkey, E. T.; Steinman, L.; Rothbard, J. B. The design, synthesis, and evaluation of molecules that enable or enhance cellular uptake: peptoid molecular transporters. *Proc. Natl. Acad. Sci.* **2000**, *97*, 13003.
- (30) Kim, W. J.; Christensen, L. V.; Jo, S.; Yockman, J. W.; Jeong, J. H.; Kim, Y. H.; Kim, S. W. Cholestryloxyloarginine delivering vascular endothelial growth factor siRNA effectively inhibits tumor growth in colon adenocarcinoma. *Mol. Ther.* **2006**, *14*, 343–350.
- (31) Kumar, P.; Wu, H.; McBride, J. L.; Jung, K. E.; Kim, M. H.; Davidson, B. L.; Lee, S. K.; Shankar, P.; Manjunath, N. Transvascular delivery of small interfering RNA to the central nervous system. *Nature* **2007**, *448*, 39–43.
- (32) Ren, Y.; Hauert, S.; Lo, J. H.; Bhatia, S. N. Identification and characterization of receptor-specific peptides for siRNA delivery. *ACS Nano* **2012**, *6*, 8620–8631.
- (33) Pham, W.; Kircher, M. F.; Weissleder, R.; Tung, C. H. Enhancing membrane permeability by fatty acylation of oligoarginine peptides. *ChemBioChem* **2004**, *5*, 1148–1151.
- (34) Galbiati, F.; Guzzi, F.; Magee, A. I.; Milligan, G.; Parenti, M. Chemical inhibition of myristoylation of the G-protein Gi1 alpha by 2-hydroxymyristate does not interfere with its palmitoylation or membrane association. Evidence that palmitoylation, but not myristoylation, regulates membrane attachment. *Biochem. J.* **1996**, *313*, 717–721.
- (35) Nelson, A. R.; Borland, L.; Allbritton, N. L.; Sims, C. E. Myristoyl-based transport of peptides into living cells. *Biochemistry* **2007**, *46*, 14771–14781.
- (36) Ifediba, M. A.; Medarova, Z.; Ng, S.-w.; Yang, J.; Moore, A. siRNA delivery to CNS cells using a membrane translocation peptide. *Bioconjugate Chem.* **2010**, *21*, 803–806.
- (37) Lee, J. H.; Engler, J. A.; Collawn, J. F.; Moore, B. A. Receptor mediated uptake of peptides that bind the human transferrin receptor. *Eur. J. Biochem.* **2001**, *268*, 2004–2012.
- (38) Van Kuik-Romeijn, P.; Platenburg, G. J. *Molecules for targeting compounds to various selected organs, tissues or tumor cells*. U.S. Patent No. 2010/0184947 A1, 2010.
- (39) Gan, L.; Johnson, D. A.; Johnson, J. A. Keap1-Nrf2 activation in the presence and absence of DJ-1. *Eur. J. Neurosci.* **2010**, *31*, 967–977.
- (40) Rouault, T. A.; Cooperman, S. Brain iron metabolism. *Semin. Pediatr. Neurol.* **2006**, *13*, 142–148.
- (41) Qian, Z. M.; Li, H.; Sun, H.; Ho, K. Targeted drug delivery via the transferrin receptor-mediated endocytosis pathway. *Pharmacol. Rev.* **2002**, *54*, 561–587.
- (42) Shayan, G.; Choi, Y. S.; Shusta, E. V.; Shuler, M. L.; Lee, K. H. Murine in vitro model of the blood-brain barrier for evaluating drug transport. *Eur. J. Pharm. Sci.* **2010**, *42*, 148–155.
- (43) Wilhelm, I.; Fazakas, C.; Krizbai, I. A. In vitro models of the blood-brain barrier. *Acta Neurobiol. Exp. (Warsaw)* **2011**, *71*, 113–128.
- (44) Leroueil, P. R.; Berry, S. A.; Duthie, K.; Han, G.; Rotello, V. M.; McNerny, D. Q.; Baker, J. R.; Orr, B. G.; Banaszak Holl, M. M. Wide varieties of cationic nanoparticles induce defects in supported lipid bilayers. *Nano Lett.* **2008**, *8*, 420–424.
- (45) Kennedy, M. T.; Pozharski, E. V.; Rakhmanova, V. A.; MacDonald, R. C. Factors governing the assembly of cationic phospholipid-DNA complexes. *Biophys. J.* **2000**, *78*, 1620–1633.
- (46) Bartlett, D. W.; Davis, M. E. Effect of siRNA nuclease stability on the in vitro and in vivo kinetics of siRNA-mediated gene silencing. *Biotechnol. Bioeng.* **2007**, *97*, 909–921.
- (47) Brown, R. C.; Morris, A. P.; O’Neil, R. G. Tight junction protein expression and barrier properties of immortalized mouse brain microvessel endothelial cells. *Brain Res.* **2007**, *1130*, 17–30.
- (48) Hanson, L. R.; Frey, W. H. Intranasal delivery bypasses the blood-brain barrier to target therapeutic agents to the central nervous system and treat neurodegenerative disease. *BMC Neurosci.* **2008**, *9*, S5.